

Wannier-Stark states in double-periodic lattices II: two-dimensional lattices

Evgeny N. Bulgakov¹, Dmitri. N. Maksimov¹, and Andrey R. Kolovsky^{1,2}

¹*Kirensky Institute of Physics, 660036 Krasnoyarsk, Russia and*

²*Siberian Federal University, 660041 Krasnoyarsk, Russia*

(Dated: February 28, 2018)

Abstract

We analyze the Wannier-Stark spectrum of a quantum particle in tilted two-dimensional lattices with the Bloch spectrum consisting of two subbands, which could be either separated by a finite gap or connected at the Dirac points. For rational orientations of the static field given by an arbitrary superposition of the translation vectors the spectrum is a ladder of energy bands. We obtain asymptotic expressions for the energy bands in the limit of large and weak static fields and study them numerically for intermediate field strength. We show that the structure of energy bands determines the rate of spreading of a localized wave packets which is the quantity measured in laboratory experiments. It is shown that wave-packet dispersion becomes a fractal function of the field orientation in the long-time regime of ballistic spreading.

I. INTRODUCTION

In our preceding work [1] we have analyzed the Wannier-Stark states (WS-states) in a tilted one-dimensional double-periodic lattice. It was shown that the spectrum of WS-states consists of two Wannier-Stark ladders that affect each other in a rather complicated way. In this paper we extend the analysis of Ref. [1] to double-periodic two-dimensional lattices or, more exactly, to two-dimensional lattices with two sublattices.

The fundamental difference of 2D lattices as compared with 1D lattices is that the Wannier-Stark spectrum and WS-states depend not only on the strength of a static field F but also on its orientation relative to the primary axes of the lattice, where one should distinguish between ‘rational’ and ‘irrational’ orientations. The former are given by an arbitrary superposition of the translation vectors and the latter comprise the remaining directions. For rational orientations WS-states are Bloch-like states in the direction orthogonal to the vector \mathbf{F} [2–4]. Thus they can be labeled by the ladder index n and the transverse quasimomentum κ . Correspondently, the energy spectrum of the system is a ladder of energy bands which are termed Wannier-Stark bands (WS-bands) in what follows. Unlike this situation, for irrational orientations the spectrum is pure point and WS-states are localized states in any direction [4].

In the work we pay special attention to physical manifestations of the structure of the energy spectrum that can be detected in a laboratory experiment, where two most favorite candidates are wave-guide arrays [5] and cold atoms in optical lattices [8]. In particular, continuous spectrum of the WS-states for rational orientations of the static field implies ballistic spreading of a localized wave packet. This effect can be easily observed for the light in a wave-guide array and, with some efforts aimed on improving resolution of the imaging system, also for cold atoms in an optical lattice. We analyze the rate of wave-packet spreading as the function of the static field magnitude and its orientation. The other quantity that can be measured in experiments with cold atoms is the total occupation of the Bloch subbands which change in time because of the interband Landau-Zener tunneling (LZ-tunneling). We shall show that knowledge of the Wannier-Stark spectrum suffices to predict different regimes of the interband dynamics.

The structure of the paper is as follows. In Sec. II we introduce the model – the tight-binding Hamiltonian of a square 2D lattice with two sublattices – and perform preliminary

numerical analysis of the Wannier-Stark spectrum. Next, in Sec. III we obtain asymptotic expressions for WS-bands in the limits of strong and weak static field. These results are used in the subsequent Sec. IV, which compares the rate of ballistic spreading calculated on the basis of WS-bands with that observed in numerical simulations of the wave-packet dynamics, and in Sec. V, which discusses Landau-Zener transitions between the Bloch subbands. The main results of the work are summarized in the concluding Sec. VI.

II. WANNIER-STARK ENERGY BANDS

As the model we shall consider a square lattice of the unit period with two different tunneling elements along the bonds and different on-site energies for the A and B sites, see Fig. 1. Notice that the primary axes of this lattice are rotated by 45 degrees with respect to the xy axes and the new period is $a = \sqrt{2}$. The Bloch spectrum of this lattice consists of two subbands with the dispersion relations $E = E_{\pm}(\kappa_x, \kappa_y)$ found as eigenvalues of the matrix

$$H_0 = \begin{pmatrix} -\delta & -J_2 - J_1(e^{-ia\kappa_x} + e^{-ia\kappa_y} + e^{-ia(\kappa_x+\kappa_y)}) \\ -J_2 - J_1(e^{ia\kappa_x} + e^{ia\kappa_y} + e^{ia(\kappa_x+\kappa_y)}) & \delta \end{pmatrix}, \quad (1)$$

where κ_x and κ_y are the Bloch wave quasimomenta. Two particular cases to be addressed in this work, are (i) $J_1 = J_2$ and $\delta \neq 0$; and (ii) $\delta = 0$ and $J_2 = 0$. In the former case two Bloch bands are separated by a finite energy gap, see Fig. 2(a), while in the latter case they touch each other at the Dirac points, see Fig. 2(b). It appears that the absence or presence of Dirac's cones in the Bloch spectrum strongly affects the Wannier-Stark spectrum and, hence, this two cases should be analyzed separately.

Let us now proceed to the tilted lattices. As it was already mentioned in Sec. I, the fundamental difference of tilted 2D lattices as compared with tilted 1D lattices is that the Wannier-Stark spectrum and WS-states depend on the field orientation, which we shall characterize by the parameter $\beta = F_x/F_y$. Alternatively, one can characterize the field orientation by the parameter

$$\tilde{\beta} = \tilde{F}_x/\tilde{F}_y,$$

where \tilde{F}_x and \tilde{F}_y are field components in the coordinate system aligned with the primary axes of the lattice. Then rational orientations corresponds to rational values of the parameter β

which also implies rational $\tilde{\beta} = r/q$ (here r and q are co-prime numbers).

To find the energy spectrum for rational $\tilde{\beta} = r/q$ we follow Ref.[2, 4] and rotate the coordinate system to align the new y -axis with the vector \mathbf{F} , and then use the plane-wave ansatz for the wave function. This results in the following eigenvalue problem

$$\begin{aligned} dF \left(l - \frac{r+q}{4} \right) \psi_l^A + \delta \psi_l^A - J_2 \psi_l^B - J_1 \left(e^{-ird\kappa} \psi_{l-q}^B - e^{iqd\kappa} \psi_{l-r}^B - e^{id(q-r)\kappa} \psi_{l-q-r}^B \right) &= E \psi_l^A, \\ dF \left(l + \frac{r+q}{4} \right) \psi_l^B - \delta \psi_l^B - J_2 \psi_l^A - J_1 \left(e^{ird\kappa} \psi_{l+q}^A - e^{-iqd\kappa} \psi_{l+r}^A - e^{-id(q-r)\kappa} \psi_{l+q+r}^A \right) &= E \psi_l^B \end{aligned} \quad (2)$$

where

$$d = \frac{a}{\sqrt{N}}, \quad a = \sqrt{2}, \quad N = r^2 + q^2.$$

One obtains the WS-bands through a sweep along the plane-wave quasimomentum κ which enters Eq. (2) as a parameter. As an example Fig. 3 shows these bands for the parameters of Fig. 2 and $F = 0.4$ and $(r, q) = (1, 0)$. [In the original coordinate system this orientation corresponds to $F_x/F_y = 1$.] It is seen in Fig. 3 that WS-bands appear in pairs and are arranged into two ladders with the step dF . As F is varied the bands change their shape in a rather complicated way. On the other hand, if we fix the quasimomentum κ , we obtain Wannier-Stark fan, see Fig. 4, which resembles that for a 1D double-periodic lattice. In particular, it is seen in Fig. 4 that energy levels of different symmetry show avoided crossing when they approach each other. If we now fix F and vary κ these avoided crossings become avoided crossings between energy bands. We would like to draw reader's attention that the discussed avoided crossings are much more pronounced in the case (ii) – we come back to this point in Sec. IIIC.

In the next section we shall analyze WS-bands in more details, focusing on their dependence on the static field F . Along with explicit form of the energy bands we shall be also interested in the following integrated characteristic,

$$A(F) = \frac{1}{2\pi} \int_0^{2\pi} v^2(\kappa) d(d\kappa), \quad v(\kappa) = \frac{\partial E}{\partial \kappa} \quad (3)$$

where $v(\kappa)$ is the the group velocity. It will be shown later on in Sec.IV that the quantity (3) determines the rate of ballistic spreading of a localized wave packet. For the purpose of future references Fig. 5 shows this quantity as the function of $1/F$.

III. STRONG VS. WEAK FIELDS

A. Strong fields

The limit of strong fields can be solved using Rayleigh-Schrödinger perturbation theory with $\epsilon = 1/F$ as the small parameter. As follows from Eq. (2), the zero-order spectrum corresponds to flat bands arranged into two ladders. Denoting by $E^{(r,q)}(\kappa)$ the perturbation correction, we have

$$E_{n,\pm}(\kappa) = dF \left(n \mp \frac{r+q}{4} \right) \pm \delta \pm E^{(r,q)}(\kappa). \quad (4)$$

The super-index (r, q) in the correction term underlines its dependence on the field orientation. It can be rigorously proved that few first terms in the perturbation series vanish and, hence, $E^{(r,q)}(\kappa) \sim \epsilon^\nu$ where ν is number of vanishings terms. For example, for the lattice (i) we have $\nu = 2$ if $F_x/F_y = 1$, $\nu = 3$ if $F_x/F_y = 1/3$, etc.. Thus, in general case the band width Δ of the WS-bands tends to zero if $F \rightarrow \infty$. Two exclusions, where the bands have a finite width in the above limit (i.e., $\nu = 0$), correspond to situations where \mathbf{F} is aligned with the x or y axis. It should be mentioned that the increment ν depends not only on the field orientation but also on the lattice geometry and for the lattice (ii) we have $\nu = 0$ if \mathbf{F} is parallel to the x axis yet $\nu = 2$ if \mathbf{F} is parallel to the y axis. It can be also shown that the first non-vanishing term of Rayleigh-Schrödinger perturbation theory gives the cosine dispersion relation for the WS-bands:

$$E^{(r,q)}(\kappa) = \Delta(F) \cos(Nd\kappa), \quad \Delta(F) \sim \frac{1}{F^\nu}. \quad (5)$$

Note that the dispersion relation $E^{(r,q)}(\kappa)$ is periodic function of κ with the period $2\pi/Nd$ but not $2\pi/d$, as one might naively expect basing on the explicit periodicity of the coefficients in Eq. (2). Finally, we mention that the functional dependence of the quantity (3) on F is obviously given by $A \sim (1/F)^{2\nu}$, see inset in Fig. 5.

B. Moderate fields

The region of applicability of the perturbation approach of Sec. III A is restricted to small values of the parameter $\epsilon = 1/F$, smaller than the position of the first peak in Fig. 5. In this subsection we discuss a more sophisticated approach which allows us consider moderate

F , where the band width Δ of WS-bands takes its maximal value. This approach is a straightforward generalization of the method used in Ref. [1] to analyze the Wannier-Stark spectrum of a quantum particle in one-dimensional lattices.

Similar to Eq. (5) in Ref. [1] we introduce the generating functions

$$Y^{A,B}(\theta) = (2\pi)^{-1/2} \sum_{l=-\infty}^{\infty} \psi_l^{A,B} \exp(il\theta) . \quad (6)$$

This reduces Eq. (2) to the system of two ordinary differential equations,

$$idF \frac{d}{d\theta} \begin{pmatrix} Y^A \\ Y^B \end{pmatrix} = G(\theta; \kappa) \begin{pmatrix} Y^A \\ Y^B \end{pmatrix} , \quad (7)$$

where

$$G(\theta; \kappa) = \begin{pmatrix} E + dF(r+q)/4 + \delta & J_2 + J_1 f(\theta; \kappa) \\ J_2 + J_1 f^*(\theta; \kappa) & E - dF(r+q)/4 - \delta \end{pmatrix} \quad (8)$$

and

$$f(\theta; \kappa) = e^{-ird\kappa} e^{-iq\theta} + e^{iqd\kappa} e^{-ir\theta} + e^{i(q-r)d\kappa} e^{-i(r+q)\theta} .$$

Equation (7) falls into the class of linear dynamical system and can be viewed as some effective two-level system driven by a three-chromatic field.

To solve Eq. (7) one can apply a variety of methods of which the Bogoliubov-Mitropolskii averaging technique proves to be the most universal [1]. For the lattice (ii) this technique was used in our recent paper [6], from which we borrow the final result. Restricting ourselves by one iteration, correction to the flat energy bands is given by

$$E^{(r,q)}(\kappa) = (J_2 - J_1) \sum_{n,m} \mathcal{J}_m(z_1) \mathcal{J}_n(z_2) \cos \left[\kappa d \frac{r^2 + q^2}{r - q} (1 + n) \right] , \quad (9)$$

where integer numbers n and m satisfy the equation $(r-q)m = -(r+q)(1+n)$ and arguments of the Bessel functions are

$$z_1 = \frac{8J_1}{Fd(r-q)} , \quad z_2 = \frac{4(J_1 + J_2)}{Fd(r+q)} .$$

Notice that, if compared with Rayleigh-Schrödinger perturbation theory, the first order Bogoliubov-Mitropolskii correction corresponds to infinite perturbation series.

Using the fact that $\mathcal{J}_n(z) \sim z^n$ for $z \ll 1$ it is easy to prove that in the limit $F \rightarrow \infty$ Eq. (9) recovers Eq. (5). However, unlike in Rayleigh-Schrödinger perturbation theory,

Eq. (9) captures oscillatory behavior of the band width $\Delta = \Delta(F)$, as well as the presence of higher harmonics in the dispersion relation. For example, in the above considered case $(r, q) = (2, 1)$ Eq. (9) takes the form

$$E^{(r,q)}(\kappa) = \pm(J_1 - J_2) [\mathcal{J}_0(z_1)\mathcal{J}_1(z_2) + \mathcal{J}_3(z_1)\mathcal{J}_0(z_2) \cos(5\kappa d) - \mathcal{J}_3(z_1)\mathcal{J}_2(z_2) \cos(5\kappa d) - \mathcal{J}_6(z_1)\mathcal{J}_1(z_2) \cos(10\kappa d) + \dots] . \quad (10)$$

Comparing Eq. (10) with the exact numerical results we found that for the parameters of Fig. 5 it correctly approximates WS-bands till $F \approx 1$, where the quantity A has the first minima.

C. Weak fields

The opposite limit of small F is more involved in the sense that the result depends on the presence of Dirac's points in the Bloch spectrum. First we shall discuss the lattice (i) where the Bloch bands are separated by the gap equal or larger than 2δ .

1. Finite gap

A finite gap insures vanishing interband LZ-tunneling in the limit $F \rightarrow 0$. Thus the spectrum of 2D WS-states can be found by using the adiabatic theorem, in full analogy with the weak field case for 1D lattices [1]. Denoting by $\tilde{\mathcal{E}}_{\pm}(\theta; \kappa)$ and $\mathbf{y}_{\pm}(\theta; \kappa)$ the eigenvalues and eigenfunctions of 2×2 matrix (8) for $E = 0$, the energy spectrum of WS-states is given by the equation

$$E_{n,\pm}(\kappa) = C_{\pm}(\kappa) + dF[n + c_{\pm}(\kappa)] , \quad (11)$$

where

$$C_{\pm}(\kappa) = \frac{1}{2\pi} \int_0^{2\pi} \tilde{\mathcal{E}}_{\pm}(\theta; \kappa) d\theta , \quad c_{\pm}(\kappa) = \frac{i}{2\pi} \int_0^{2\pi} \mathbf{y}_{\pm}^T(\theta; \kappa) \frac{d}{d\theta} \mathbf{y}_{\pm}(\theta; \kappa) d\theta' \quad (12)$$

are the dynamical and geometrical phases, respectively. Equation (11) contains the transverse quasimomentum κ as a parameter. In fact, one can related this quasimomentum and the constants (12) to the Bloch spectrum $E_{\pm}(\kappa_x, \kappa_y)$ of the system. To do this we rotate the axis in the quasimomentum space to align the new κ'_y axis with the vector \mathbf{F} of the static field. Then the transverse quasimomentum κ is associated with κ'_x and the constant $C_{\pm}(\kappa)$

coincide in the limit $F \rightarrow 0$ with the mean energy of the Bloch subbands along the line parallel to \mathbf{F} :

$$\lim_{F \rightarrow 0} C_{\pm}(\kappa) = \frac{1}{2\pi} \int_0^{2\pi} E_{\pm}(\kappa, \kappa'_y) d(\kappa'_y) \equiv \pm E^{(r,q)}(\kappa). \quad (13)$$

Let us discuss the dispersion relation (13) in some more details. The left panel in Fig. 6 shows this dispersion relation for three different orientations of the static field: $(r, q) = (1, 0)$, $(r, q) = (1, 1)$, and $(r, q) = (2, 1)$. It is seen that $E^{(r,q)}(\kappa)$ rapidly converges to a flat band when r and q are increased. More elaborated numerical analysis shows that this convergence is exponentially fast, see right panel in Fig. 6. Thus, for most of the field orientations the band width Δ takes an exponentially small value in the limit $F \rightarrow 0$.

2. Dirac's cones

As seen in Fig. 5, for the lattice (i) the quantity (3), which characterizes the width of WS-bands, takes a constant value as F is decreased. Obviously, this is a manifestation of transition to the adiabatic regime of interband LZ-tunneling. This result, however, does not hold for the lattice (ii) where the Bloch subbands are connected at the Dirac points. In this situation we have non-negligible LZ-tunneling for arbitrary small F and arbitrary field orientations [7]. Correspondently, the function $A = A(F)$ does not take a constant value in the limit of small F .

To study the interband LZ-tunneling we consider a delocalized initial condition given by a Bloch wave. For this initial condition the problem reduces to solving the Schrödinger equation

$$i \frac{d}{dt} \begin{pmatrix} \psi^A \\ \psi^B \end{pmatrix} = H(t) \begin{pmatrix} \psi^A \\ \psi^B \end{pmatrix}, \quad (14)$$

where $H(t)$ is obtained from the Hamiltonian (1) by substituting $\kappa_{x,y} \rightarrow \kappa_{x,y} - \tilde{F}_{x,y}t$. Notice that the solution depends on the initial quasimomenta. Thus, at any given time populations of the Bloch sub-bands are functions of κ_x and κ_y , i.e., $P_{\pm}(t) = P_{\pm}(\kappa_x, \kappa_y; t)$. Figure 7 shows snapshots of $P_+(\kappa_x, \kappa_y; t)$ for the lattice (ii) where initially only the lower band was populated – a setup corresponding to Fermi particles with the Fermi energy at $E = 0$ [8]. It is seen in the figure that the particles are transmitted into the upper band through the cones. In addition to Fig. 7, Fig. 8 compares the averaged over the time total populations of the upper band for the lattice (i) and (ii). It is seen that in the former case $\langle P_+ \rangle \propto \exp(-1/F)$

while in the latter case $\langle P_+ \rangle \propto \text{const}$. This explains qualitative difference between the lattice (i) and (ii) in the weak field limit.

IV. BALLISTIC SPREADING OF A LOCALIZED WAVE PACKET

The continuous spectrum of WS-states implies ballistic spreading of a localized wave packet where, asymptotically, the second moment of the packet grows quadratically in time:

$$M_2(t) \rightarrow Bt^2, \quad M_2(t) = \sum_{l,m} (l^2 + m^2) |\psi_{l,m}(t)|^2.$$

For the lattice (i) this behavior is illustrated in Fig. 9 where initially single site at the lattice origin was populated. We mention that we shall get essentially the same result if we chose a finite-width incoherent packet as the initial condition. Approximating numerical data in Fig. 9(a) by a straight line we extract coefficient B .

Let us now evaluate the second momentum analytically. For simplicity we shall consider the case $(r, q) = (1, 1)$ where the wave packet spreads in the x directions. Expanding the initial wave function over the basis of WS-states we obtain,

$$\psi_{l,m}(t) = \sum_n \int d\kappa a_n(\kappa) \Psi_{l,m}^{(n,\kappa)} e^{-i[dFn+E(\kappa)]t}, \quad (15)$$

where $a_n(\kappa)$ are the expansion coefficients and we omit plus-minus index for two different Wannier-Stark ladders. Because WS-states are Bloch-like states in the x direction the following decomposition is valid: $\Psi_{l,m}^{(n,\kappa)} = b_m^{(n)}(\kappa) e^{i\kappa l}$. Next, using the identity $l\Psi_{l,m}^{(n,\kappa)} = -i\mathbf{b}_m^{(n)}(\kappa) d e^{i\kappa l} / d\kappa$ one can prove the following intermediate result:

$$l\psi_{l,m} \approx t \sum_n \int d\kappa a_n(\kappa) \frac{\partial E}{\partial \kappa} \Psi_{l,m}^{(n,\kappa)} e^{-i[dFn+E(\kappa)]t}. \quad (16)$$

To obtain the last equation we used integration by parts and kept only the term which grows in time. With the help of Eq. (16) the second moment is given by

$$M_2(t) \approx \sum_l |l\psi_{l,m}(t)|^2 = t^2 \sum_n \int d\kappa |a_n(\kappa)|^2 \left(\frac{\partial E}{\partial \kappa} \right)^2.$$

Finally, using the normalization condition $\sum_n \int d\kappa |a_n(\kappa)|^2 = 1$, we estimate the second moment as

$$M_2(t) \sim At^2, \quad (17)$$

where the coefficient A is defined in Eq. (3). Figure 11 compares the rate of ballistic spreading $B = B(F)$, which was obtained by using the wave-packet simulations, with the quantity $A = A(F)$, which was calculated by using the dispersion relation of WS-states. An excellent agreement is noticed, in spite of a number of approximations that are used to derive Eq. (17).

It is interesting to compare the wave-packet dispersion $\sigma(t) = \sqrt{M_2(t)}$ for different orientations of the vector \mathbf{F} , see Fig. 11. In the considered case of weak field $F < J$ the short-time dynamics is defined by the ballistic spreading of a localized packet for $F = 0$. However, for longer time the system ‘begins to feel’ the static field. At this stage it differentiates between rational and irrational orientations. For rational orientations the packet continues to spread in the direction orthogonal to the vector \mathbf{F} , while for irrational orientations dispersion $\sigma(t)$ saturates at some level. Considering the dispersion as the function of field orientation $\theta = \arctan(F_x/F_y)$, we observe development of a fractal structure where each peak is associated with some rational $\beta = F_x/F_y$ (see Fig. 12).

V. INTERBAND DYNAMICS

As mentioned in Sec. I, cold atoms in optical lattices offers a possibility for measuring populations of the Bloch subbands. In this section we discuss population dynamics and relate it to the energy spectrum of WS-states. We shall consider two different initial conditions: Bloch wave with zero quasimomentum (i.e., the ground state of the system) and equal occupation of all quasimomentum states belonging to the lower subband. These initial conditions are realized in experiments with noninteracting Bose and Fermi atoms, respectively. On the formal level the latter case implies analysis of the population dynamics for arbitrary initial quasimomentum, followed by averaging over the Brillouin zone.

The thin solid lines in Fig. 13 show the total population of the upper Bloch band $P_+ = P_+(t)$ for the bosonic initial condition, where two panels refer to rational orientation $F_x/F_y = 1/3$ and irrational $F_x/F_y = (\sqrt{5} - 1)/4 \approx 1/3$. It is seen that for the rational orientation $P_+(t)$ is (almost) periodic process while it is a complex quasiperiodic process for the irrational orientation. This is explained by the fact that one-dimensional dispersion relation $E_{\pm}(t) = E_{\pm}(\kappa_x + F_x t, \kappa_y + F_y t)$ – the quantity which implicitly enters the Schrödinger Eq. (14) – is periodic function of time for rational $\beta = F_x/F_y$ and quasiperiodic function for irrational β . Thus for rational β one has chance to observe periodic population dynamics similar to

periodic Stückelberg oscillations in one-dimensional lattices.

Remarkably, for the fermionic initial condition situation is inverted. Because of continuous spectrum of WS-states for rational β , the averaging over the Brillouin zone leads to irreversible decay of oscillations, so that population of the upper band stabilizes at some level. On the contrary, for irrational β the spectrum of WS-states is discrete. As a consequence, the characteristic quasiperiod of $P_+(t)$ is the same for any initial quasimomentum and the averaging over the Brillouin zone single out this quasiperiod, see thick line in Fig. 13(b).

VI. CONCLUSIONS

In the work we analyzed the energy spectrum of a quantum particle in tilted double-periodic lattices with the square symmetry. It was shown that for rational orientations of a static field, $\tilde{F}_x/\tilde{F}_y = r/q$ where r and q are co-prime numbers, the spectrum consists of two ladders of energy bands termed the Wannier-Stark bands (WS-bands). We obtained asymptotic expressions for WS-bands in the limit of strong and weak fields and numerically analyze these bands for intermediate F .

As the main result we proved that WS-bands determine the rate of ballistic spreading of a localized wave-packet, which is the quantity that can be directly measured in a laboratory experiment. Importantly, this spreading takes place only in the direction orthogonal to the vector \mathbf{F} . The underlying phenomenon behind this effect is the interband Landau-Zenner tunneling (LZ-tunneling) between Bloch subbands [12]. Thus the present work can be considered as an analysis of interband LZ-tunneling in two-dimensional lattices – the problem which has attracted much attention in 1D lattices [13–16].

With respect to the wave-packet spreading the results can be summarized as follows. In the strong field limit the rate of ballistic spreading A obeys universal law $A \sim 1/F^\nu$ where the increment ν is an integer number uniquely determined by the lattice geometry and field orientation relative to the primary axes of the lattice. In the opposite weak field limit the rate A also shows universal behavior, however, only in the case where the Bloch spectrum of the system does not contain Dirac points. If it is the case, A becomes independent of F and depends only on the lattice geometry and field orientation. In terms of LZ-tunneling these two asymptotic regimes correspond to nearly diabatic and adiabatic interband dynamics. For intermediate F the interband dynamics is neither diabatic no adiabatic and the rate A

is a complicated function of the field magnitude, showing a number of peaks and deeps. As argued in our recent paper [6], the oscillatory behavior of $A = A(F)$ is a 2D analogue of the phenomenon of dynamic localization in tilted and driven 1D lattices [9–11].

To avoid confusions, we would like to stress that we considered 2D lattices with the Bloch spectrum consisting of two subbands and all above effects are absent in ‘simple’ lattices with single Bloch band. (Here ‘simple’ does not implies simplicity of the Wannier-Stark problem, see Refs. [17, 18], for example.) In the latter lattices the wave packet stay localized for any orientation of the vector \mathbf{F} , excluding the trivial case where \mathbf{F} is aligned with one of two primary axis of the lattice. Unlike this situation, the wave packet in double-periodic 2D lattices spreads ballistically for every rational orientation $\theta = \arctan(r/q)$ with a well defined rate $A = A(F, \theta)$. As a consequence, the wave-packet dispersion $\sigma = \sigma(t, \theta)$ becomes a fractal function of θ in course of time. This effect was earlier predicted in Ref. [19] for strongly decaying systems where WS-states are quantum resonances. Here we found it in not-decaying systems, which should facilitate its experimental observation.

The authors acknowledge financial support of of Russian Academy of Sciences through the SB RAS integration project No.29 *Dynamics of atomic Bose-Einstein condensates in optical lattices* and the RFBR project No.15-02-00463 *Wannier-Stark states and Bloch oscillations of a quantum particle in a generic two-dimensional lattice*.

-
- [1] D.N.Maksimov, E.N.Bulgakov, and A.R.Kolovsky, *Wannier-Stark states in one-dimensional double-periodic lattices*, arXiv:1409.3624 (2014).
 - [2] T. Nakanishi, T. Ohtsuki, and M. Saitoh, *Stark ladders in two-dimensional tight-binding lattice*, J. of Phys. Soc. Japan **62**, 2773 (1993).
 - [3] M. Glück, F. Keck, A. R. Kolovsky, and H. J. Korsch, *Wannier-Stark states of a quantum particle in 2D lattices*, Phys. Rev. Lett. **86**, 3116 (2001).
 - [4] A.R.Kolovsky and E.N.Bulgakov, *Wannier-Stark states and Bloch oscillations in the honeycomb lattice*, Phys. Rev. A **87**, 033602 (2013).
 - [5] G.Corrielli, A.Crespi, G.Della Valle, S.Longhi, and R.Osellame, *Fractional Bloch oscillations in photonic lattices*, Nature Comm. **4**, 1555 (2013).
 - [6] E.N.Bulgakov and A.R.Kolovsky, *Induced tunneling and localization for a quantum particle in*

- tilted two-dimensional lattices*, Phys. Rev. B **89**, 035116 (2014).
- [7] Lih-King Lim, J.-N. Fuchs, and G. Montambaux, *Bloch-Zener oscillations across a merging transition of Dirac points*, Phys. Rev. Lett. **108**, 175303 (2012)
- [8] L. Tarruell, D. Greif, T. Uehlinger, G. Jotzu, and T. Esslinger, *Creating, moving and merging Dirac points with a Fermi gas in a tunable honeycomb lattice*, Nature **483**, 302 (2012).
- [9] X.-G. Zhao, *Dynamic localization conditions of a charged particle in a dc-ac electric field*, Phys. Lett. A **155**, 299 (1991).
- [10] S. Longhi, M. Marangoni, M. Lobino, R. Ramponi, P. Laporta, E. Cianci, and V. Foglietti, *Observation of dynamic localization in periodically curved waveguide arrays*, Phys. Rev. Lett. **96**, 243901 (2006).
- [11] A. Eckardt, M. Holthaus, H. Lignier, A. Zenesini, D. Ciampini, O. Morsch, and E. Arimondo, *Exploring dynamic localization with a Bose-Einstein condensate*, Phys. Rev. A **79**, 013611 (2009).
- [12] A. R. Kolovsky and H. J. Korsch, *Bloch oscillations of cold atoms in 2D optical lattices*, Phys. Rev. A **67**, 063601 (2003).
- [13] B. Breid, D. Witthaut, and H. J. Korsch, *Bloch-Zener oscillations*, New J. Phys. **8**, 110 (2006).
- [14] F. Dreisow, A. Szameit, M. Heinrich, T. Pertsch, S. Nolte, A. Tünnermann, and S. Longhi, *Bloch-Zener oscillations in binary superlattices*, Phys. Rev. Lett. **102**, 076802 (2009).
- [15] S. Kling, T. Salger, C. Grossert, and M. Weitz, *Atomic Bloch-Zener oscillations and Stückelberg interferometry in optical lattices*, Phys. Rev. Lett. **105**, 215301 (2010).
- [16] P. Plötz and S. Wimberger, *Stückelberg-interferometry with ultra-cold atoms*, EPJ D **65**, 199 (2011).
- [17] F. Keck and H. J. Korsch, *Infinite-variable Bessel functions in two-dimensional Wannier-Stark systems*, J. Phys. A: Math. Gen. **35**, L105 (2002).
- [18] A. Szameit, T. Pertsch, S. Nolte, A. Tünnermann, U. Peschel, and F. Lederer, *Optical Bloch oscillations in general waveguide lattices*, J. Opt. Soc. Am. B **24**, 2632 (2007).
- [19] M. Glück, A. R. Kolovsky, and H. J. Korsch, *Fractal stabilization of Wannier-Stark resonances*, Europhys. Lett. **51**, 255 (2000).

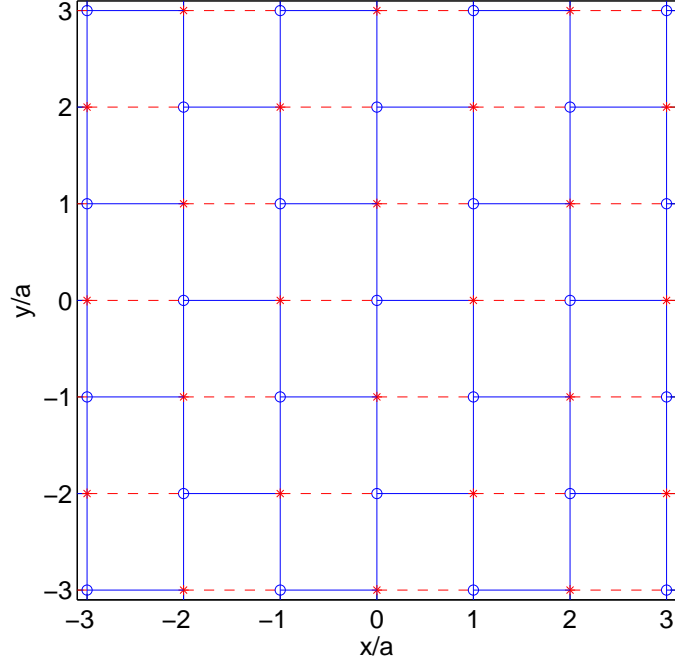


FIG. 1: The tight-binding model: a quantum particle has on-site energies $\pm\delta$ for the A (open circles) and B (asterisks) sites and can tunnel out a given lattice site to the nearest site with the tunneling rate J_1 (solid line bonds) and J_2 (dashed line bonds).

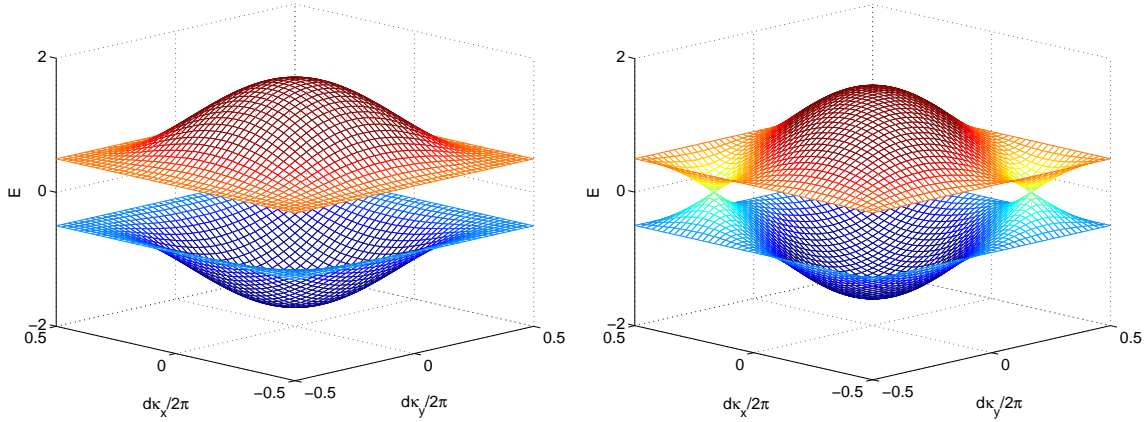


FIG. 2: Bloch bands of the double-periodic lattice shown in Fig. 1 for $J_1 = J_2 = 0.4$ and $\delta = 0.5$ (the lattice (i) in what follows), left panel , and $J_1 = 0.5$ and $J_2 = \delta = 0$ (the lattice (ii) in what follows), right panel.

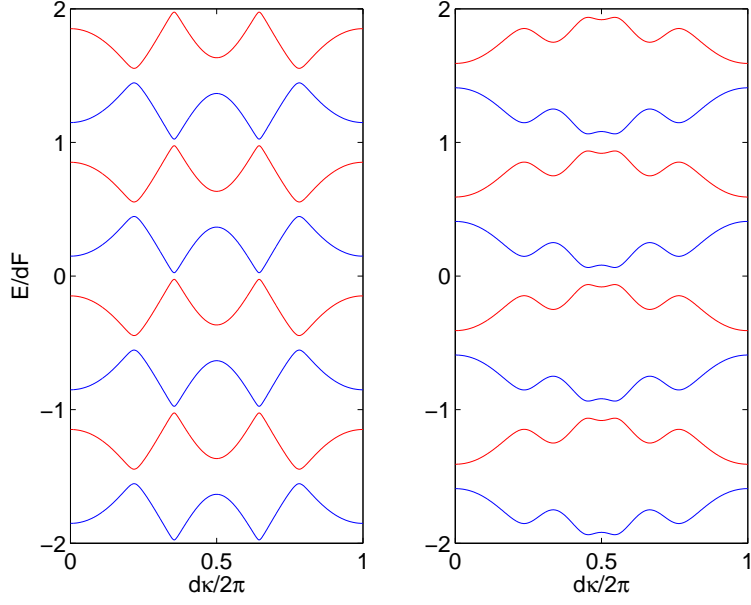


FIG. 3: Ladders of Wannier-Stark energy bands for the lattice (i), left panel, and the lattice (ii), right panel. Parameters of the static field are $F = 0.4$ and $F_x/F_y = 1$.

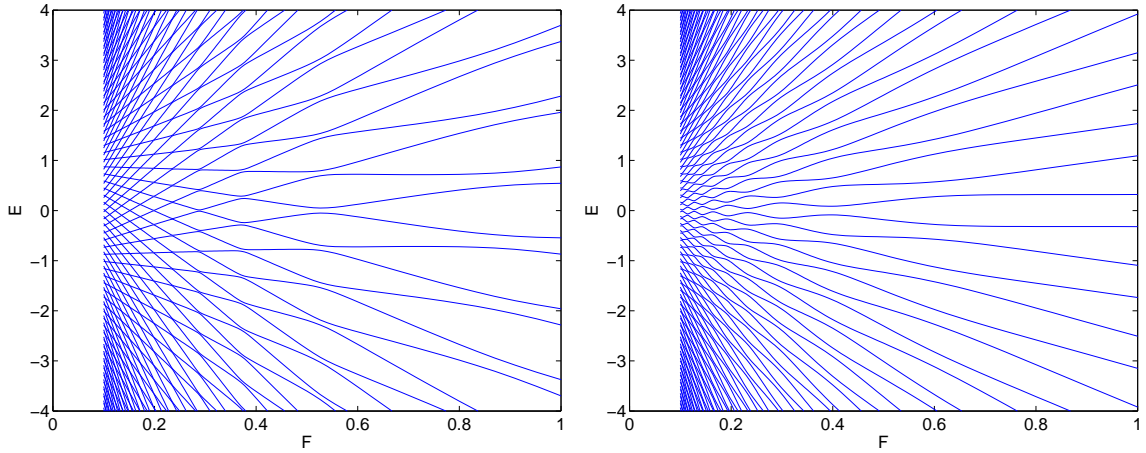


FIG. 4: Wannier-Stark fan for the lattice (i), left panel, and (ii), right panel. The transverse quasimomentum $\kappa = \pi/2d$ (i.e., $d\kappa/2\pi = 0.25$), $F = 0.4$ and $F_x/F_y = 1$.

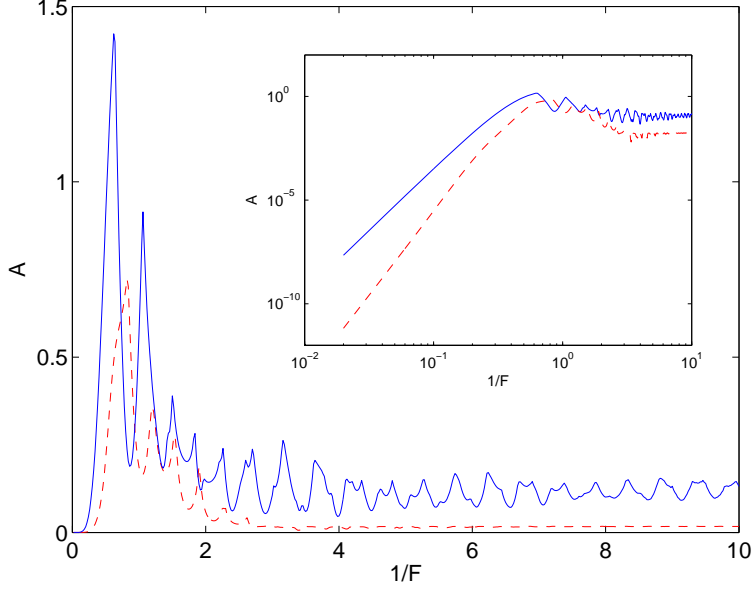


FIG. 5: The quantity A as the function of $1/F$ for the lattice (i), dashed line, and the lattice (ii), solid line. Field orientation is $F_x/F_y = 1/3$ or $(r, q) = (2, 1)$. The inset shows the same functions in the logarithmic scale.

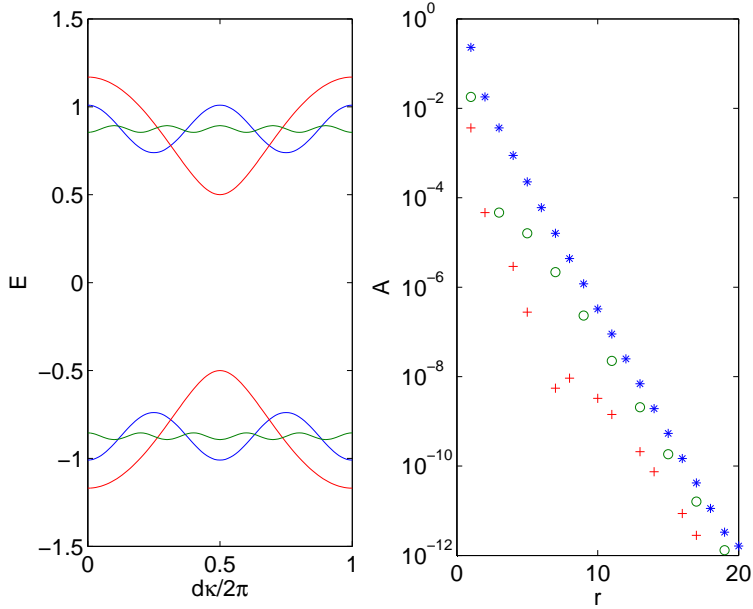


FIG. 6: Left panel: Dispersion relations $E^{(r,q)}(\kappa)$ in the limit $F \rightarrow 0$ for the lattice (i) and $(r, q) = (1, 0)$, dash-dotted line, $(r, q) = (1, 1)$, dashed line, and $(r, q) = (2, 1)$, solid line. Right panel: The quantity (3) calculated on the basis of the limiting dispersion relation for $1 \leq r \leq 20$ and $q = 1$, asterisks, $q = 2$, open circles, and $q = 3$, pluses.

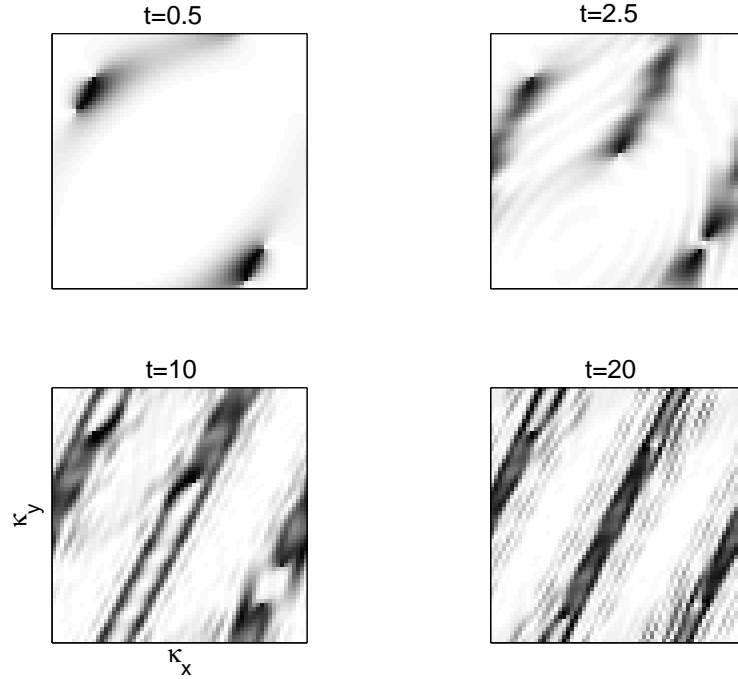


FIG. 7: Snapshots of $P_+(\kappa_x, \kappa_y; t)$ for the lattice (ii) where initially the lower Bloch subband is completely populated. Parameters are $F = 0.2$, and $F_x/F_y = 1/3$, the time is measured in the units of $T_J = 2\pi/J_1$.

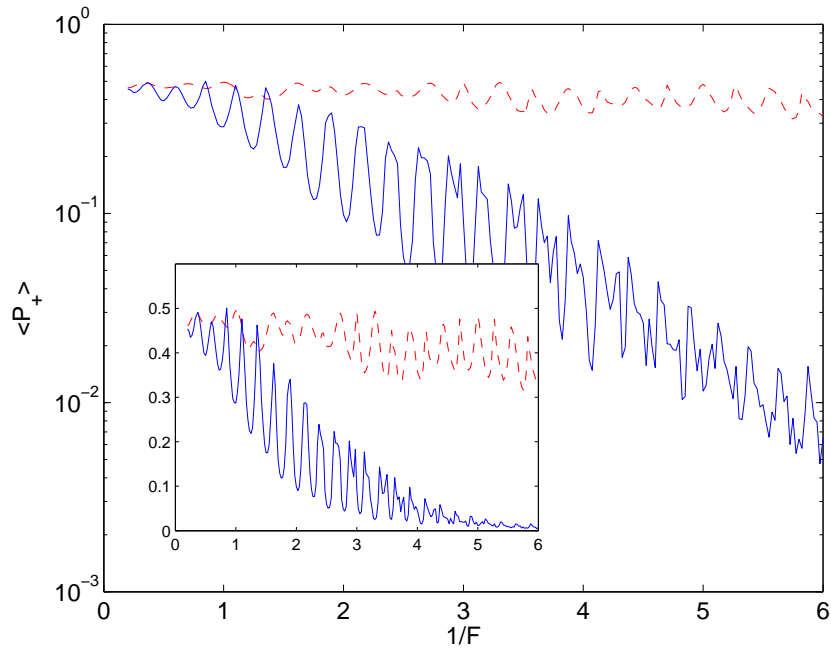


FIG. 8: Time-averaged population of the upper band as the function of $1/F$ for the lattice (i), solid line, and the lattice (ii), dashed line, in the linear (inset) and logarithmic (main panel) scales.

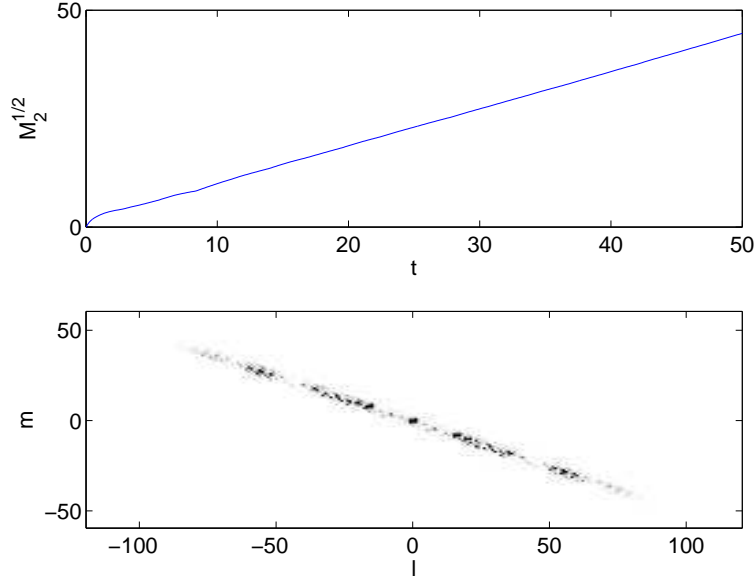


FIG. 9: Upper panel: Square root of the second moment as the function of time. Lower panel: Populations of the lattice sites $|\psi_{l,m}|^2$ at $t = 50T$, $T = 2\pi$. Parameters are $F = 0.8$, and $(r, q) = (2, 1)$.

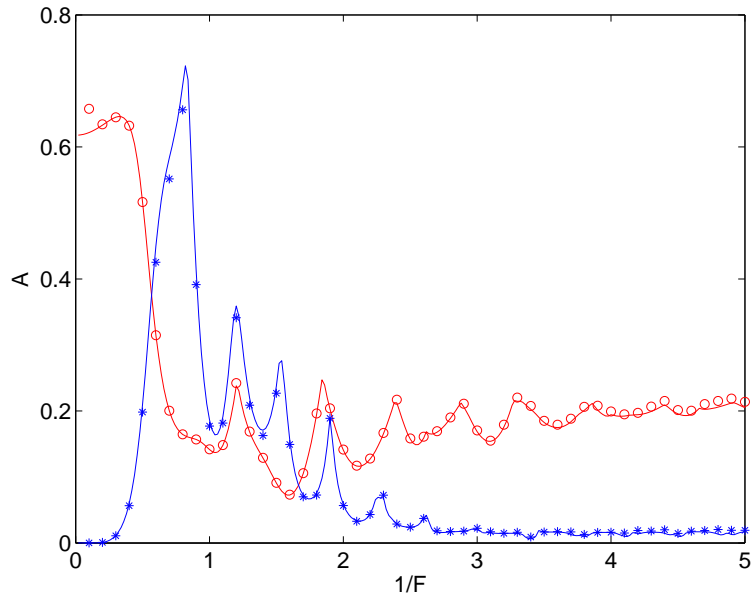


FIG. 10: Rates of ballistic spreading as the function of $1/F$, symbols, as compared to the analytic estimate (3), solid lines. The field orientation is $F_x/F_y = 0$, open circles, and $F_x/F_y = 1/3$, asterisks.

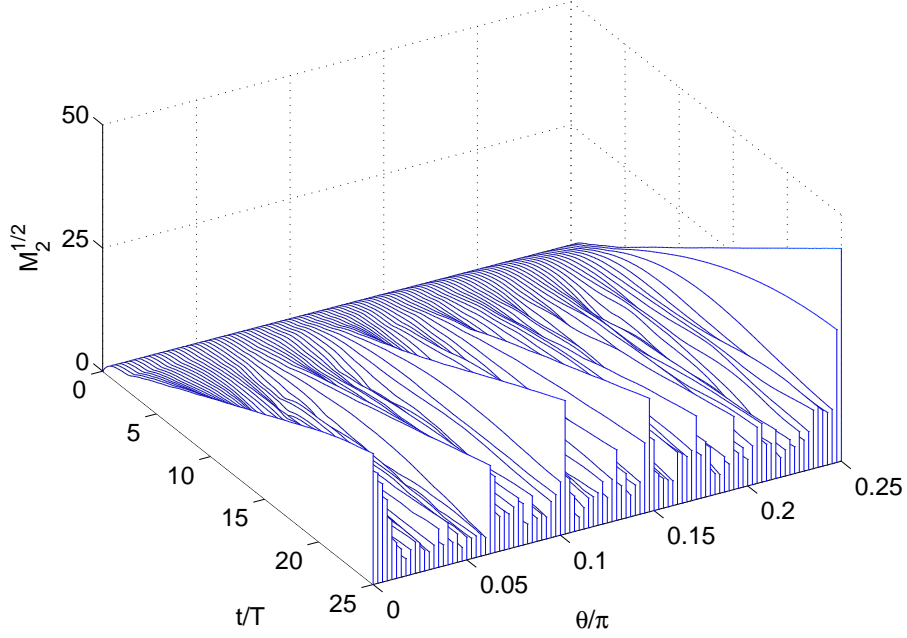


FIG. 11: Dispersion $\sigma(t) = \sqrt{M_2(t)}$ as the function of time for several orientations of the static field $\theta = \arctan(F_x/F_y)$. Parameters are: lattice (i), $F = 0.8$.

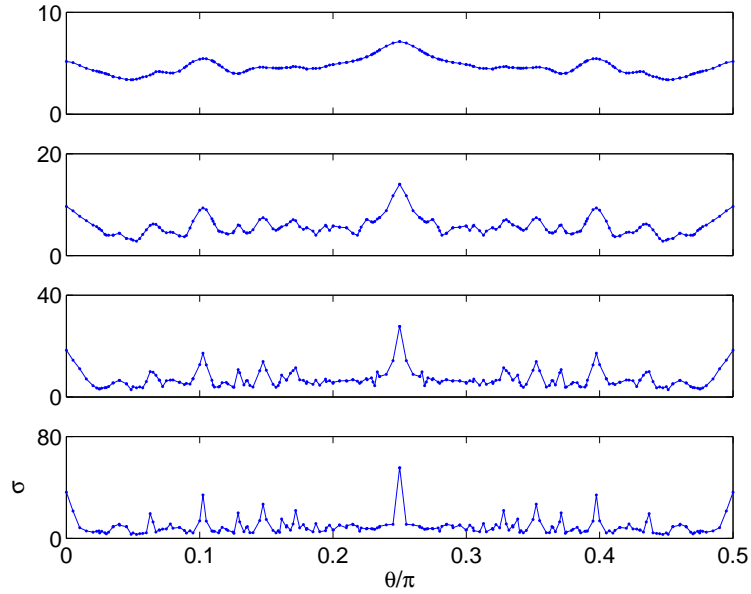


FIG. 12: Dispersion $\sigma(t) = \sqrt{M_2(t)}$ as the function of θ for four different times which differ by factor 2 for the nearest panels.

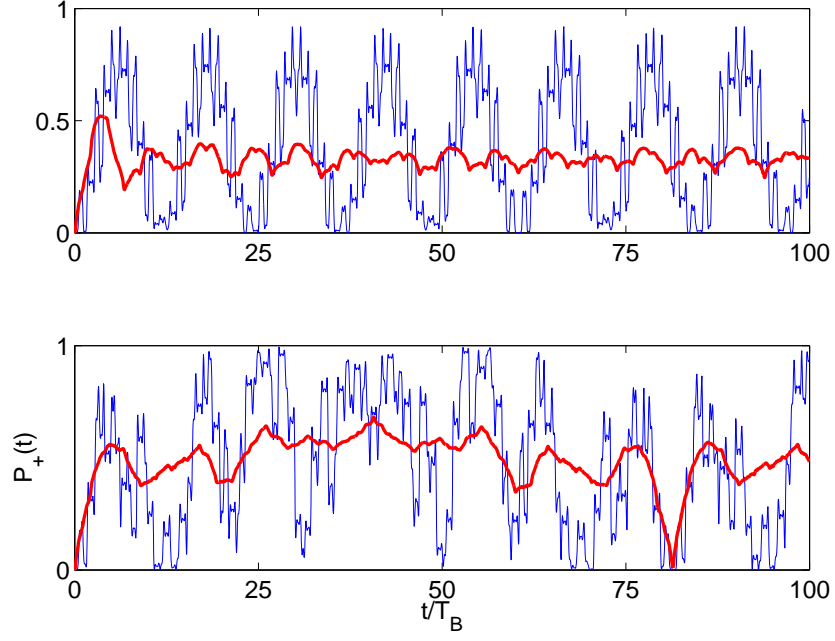


FIG. 13: Population of the upper band as the function of time for $\beta = 1/3$, upper panel, and $\beta = (\sqrt{5} - 1)/4 \approx 1/3$, lower panel. The solid and dashed lines refer to Bose and Fermi atoms, respectively (see text). The other parameters are: the lattice (i) and $F = 0.5$.